



Supplement of

Seasonality of the Quasi-biennial Oscillation signal in water vapor in the tropical stratosphere

Qian Lu et al.

Correspondence to: Jian Rao (raojian@nuist.edu.cn)

The copyright of individual parts of the supplement might differ from the article licence.

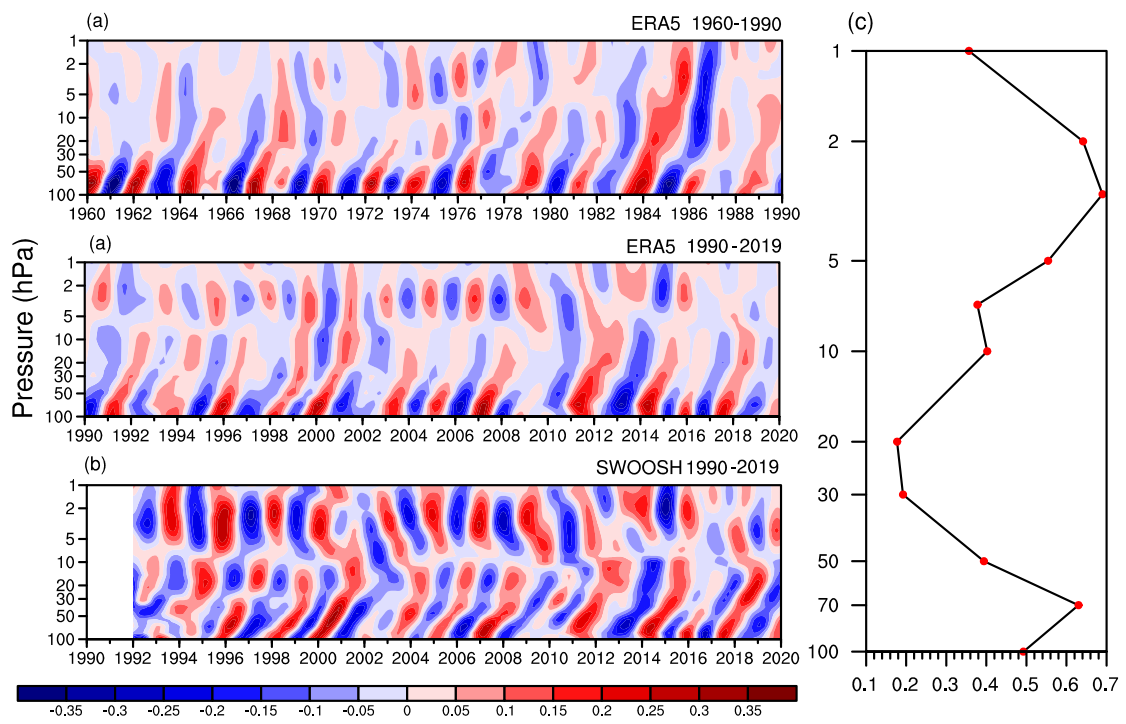


Figure S1. The same as Fig.2, but below 1 hPa.

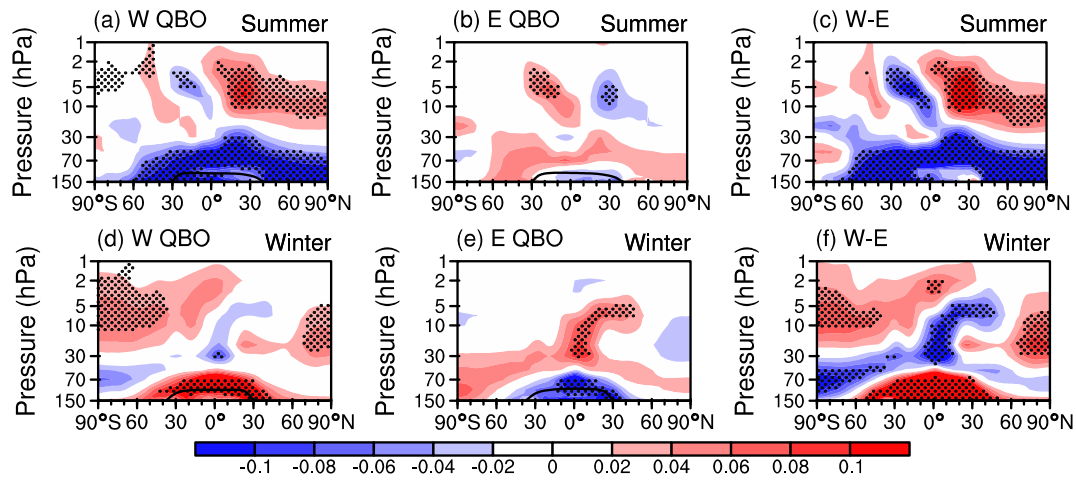


Figure S2. Water vapor anomalies under different QBO phases in the northern winter and summer from 1959–2019 for ERA5 reanalysis (mass mixing ratio, unit: ppm), respectively. The black line marks the tropopause for QBO composite. (a) Composite of QBO westerly in northern summer. (b) Composite of QBO easterly in northern summer. (c) The difference between a and b. (d–f) As in a–c, but for northern winter. Dots denote statistical significance at the 95% confidence level based on Student t-test.

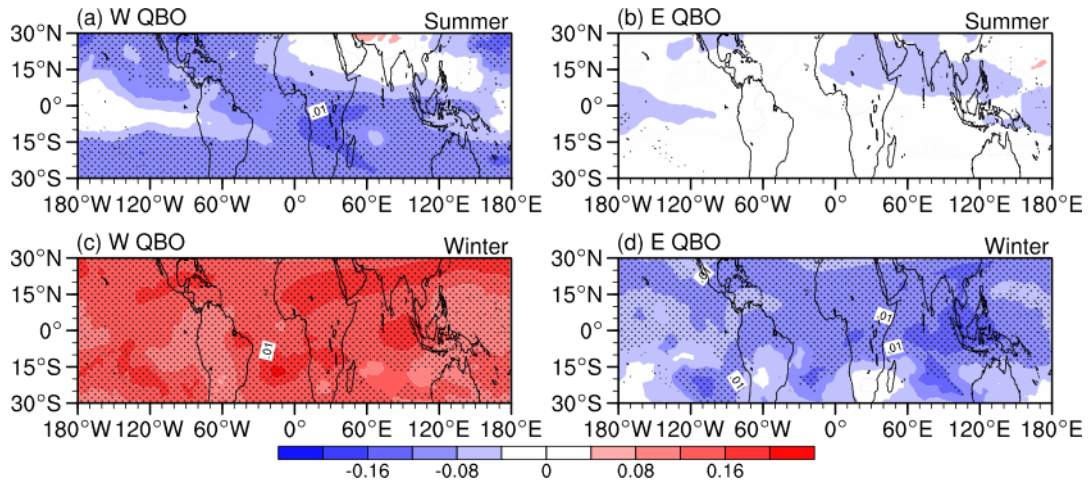


Figure S3. Distribution of WV anomalies at 100 hPa under different QBO phases in northern winter and summer from 1959–2019 for ERA5 reanalysis (mass mixing ratio, unit: ppm), respectively. (a) Composite of QBO westerly in northern summer. (b) Composite of QBO easterly in northern summer. (c, d) As in (a, b), but for northern winter.

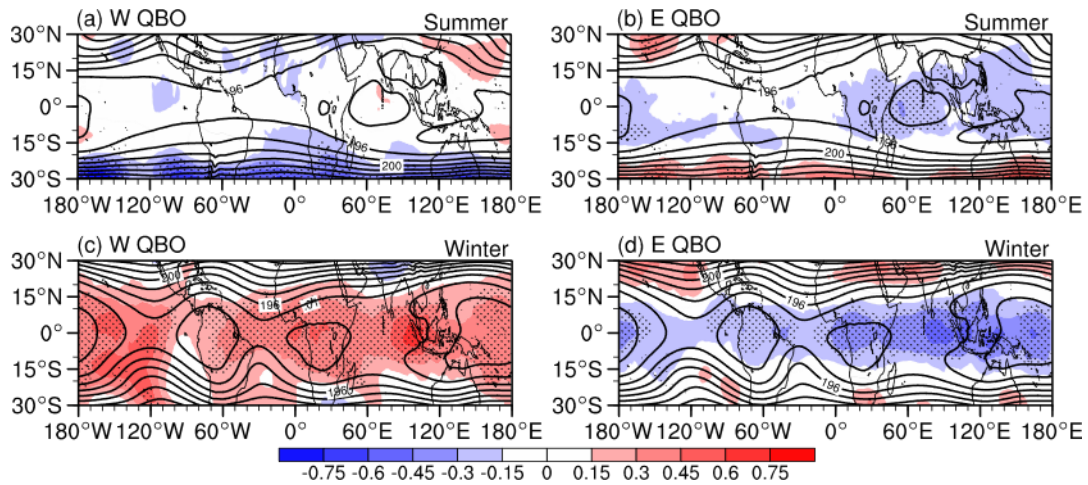


Figure S4. Temperature anomalies at 100 hPa under different QBO phases in northern winter and summer from 1959–2019 for ERA5 reanalysis (shadings; unit: K), respectively. (a) Temperature anomalies during the QBO westerly phase in the northern summer. (b) Temperature anomalies during the QBO easterly phase in the northern summer. (c, d) As in a, b but for temperature anomalies for the northern winter. Contours show the temperature climatology in winter and summer (contour interval: 2), and dots mark the composite anomalies at the 95% confidence level.

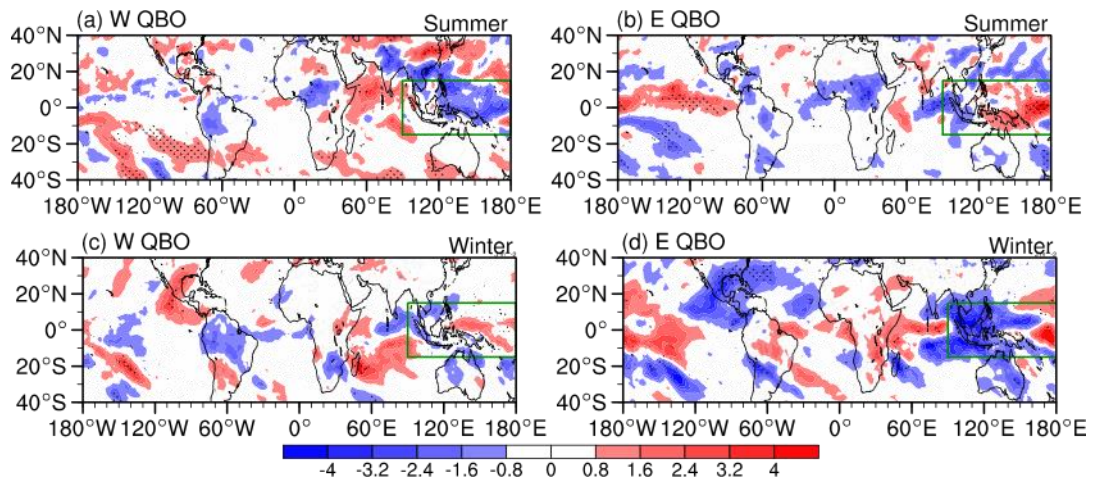


Figure S5. Outgoing longwave radiation (OLR) anomalies under different QBO phases in northern winter and summer from 1959–2019 for ERA5 reanalysis (unit: $W m^{-2}$), respectively. (a) OLR anomalies during the QBO westerly phase in the northern summer. (b) OLR anomalies during the QBO easterly phase in the northern summer. (c, d) As in a, b but for OLR anomalies for the northern winter. Dots mark the composite anomalies at the 95% confidence level.

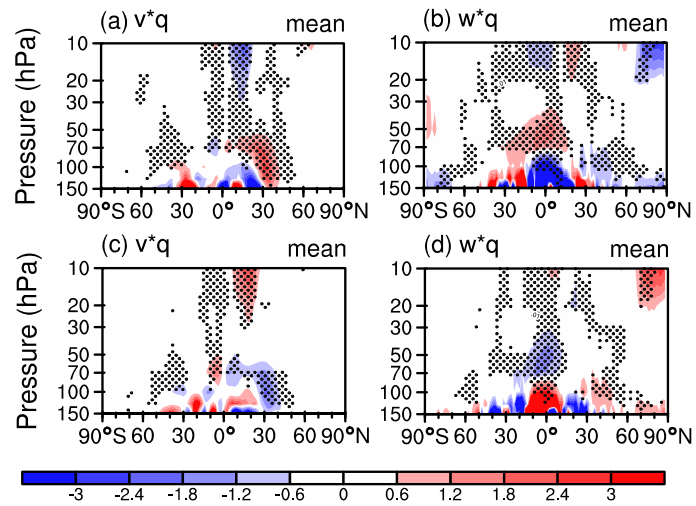


Figure S6. Diagnosis of the mean advection of water vapor from 1959–2019 for ERA5 reanalysis. (a) Meridional mean advection during the QBO westerly phase (ppb day⁻¹). (b) Vertical mean advection during the QBO westerly phase (ppb day⁻¹). (c,d) The same as in (a,b) but for the QBO easterly phase.

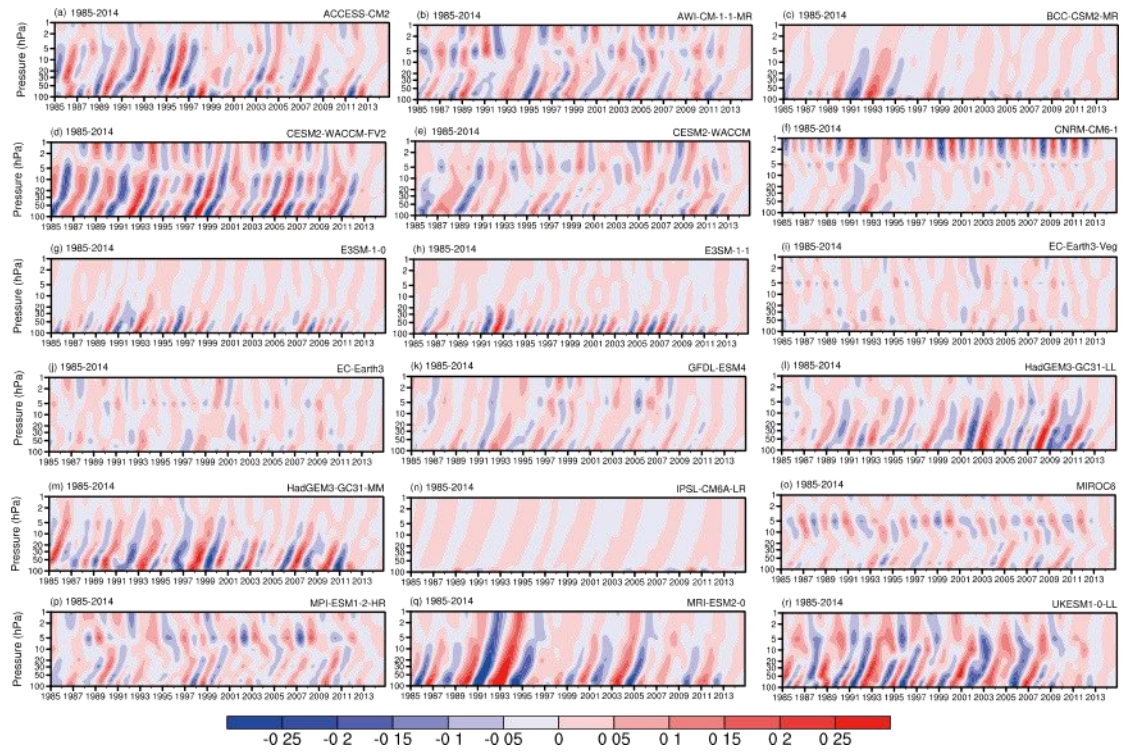


Figure S7. The same as Fig.10, but below 1 hPa.

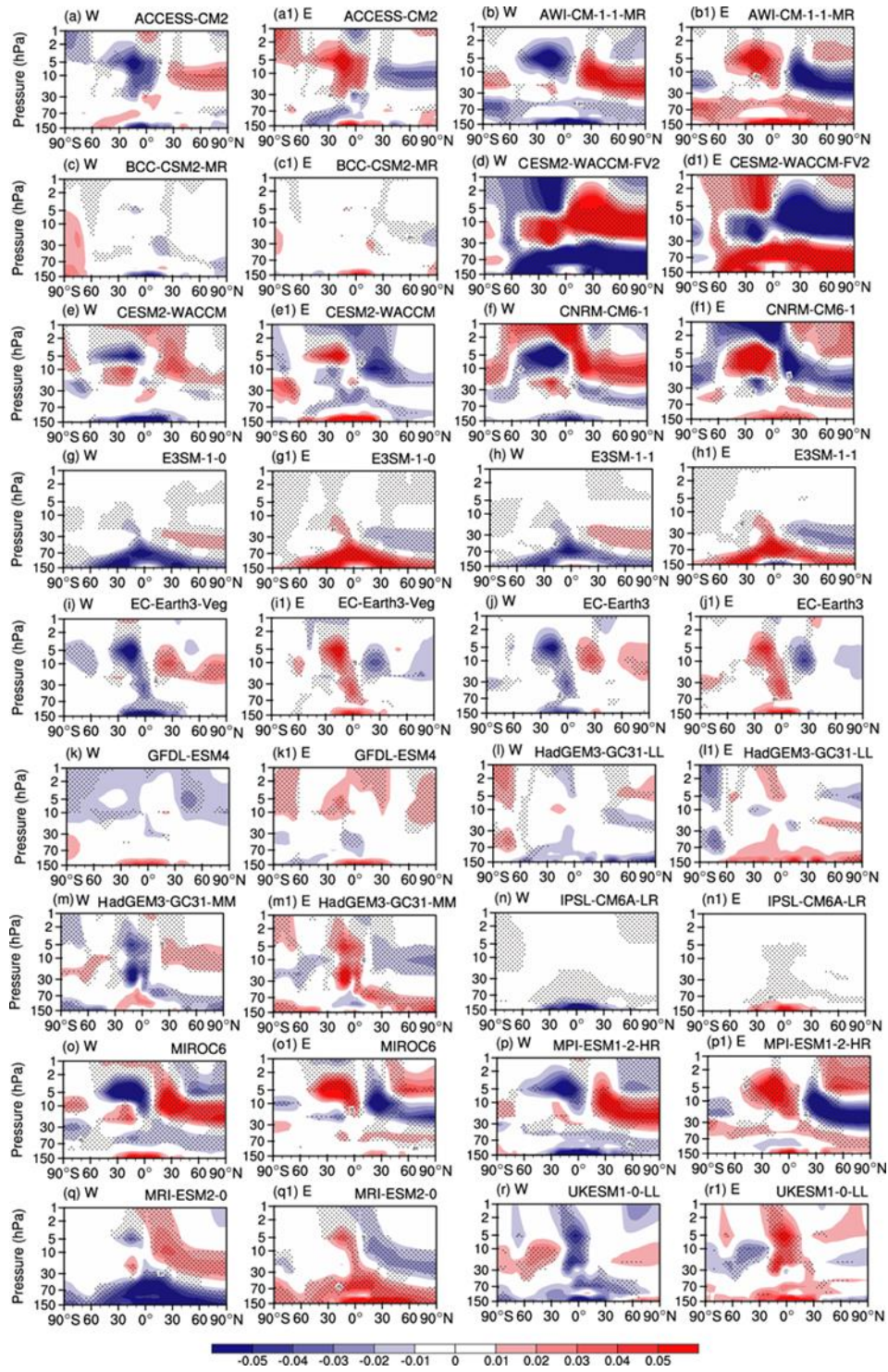


Figure S8. As in Figure S2, but for composite water vapor anomalies under different QBO phases in the northern summer (unit: ppm), respectively, for 18 CMIP6 models from 1959–2014.

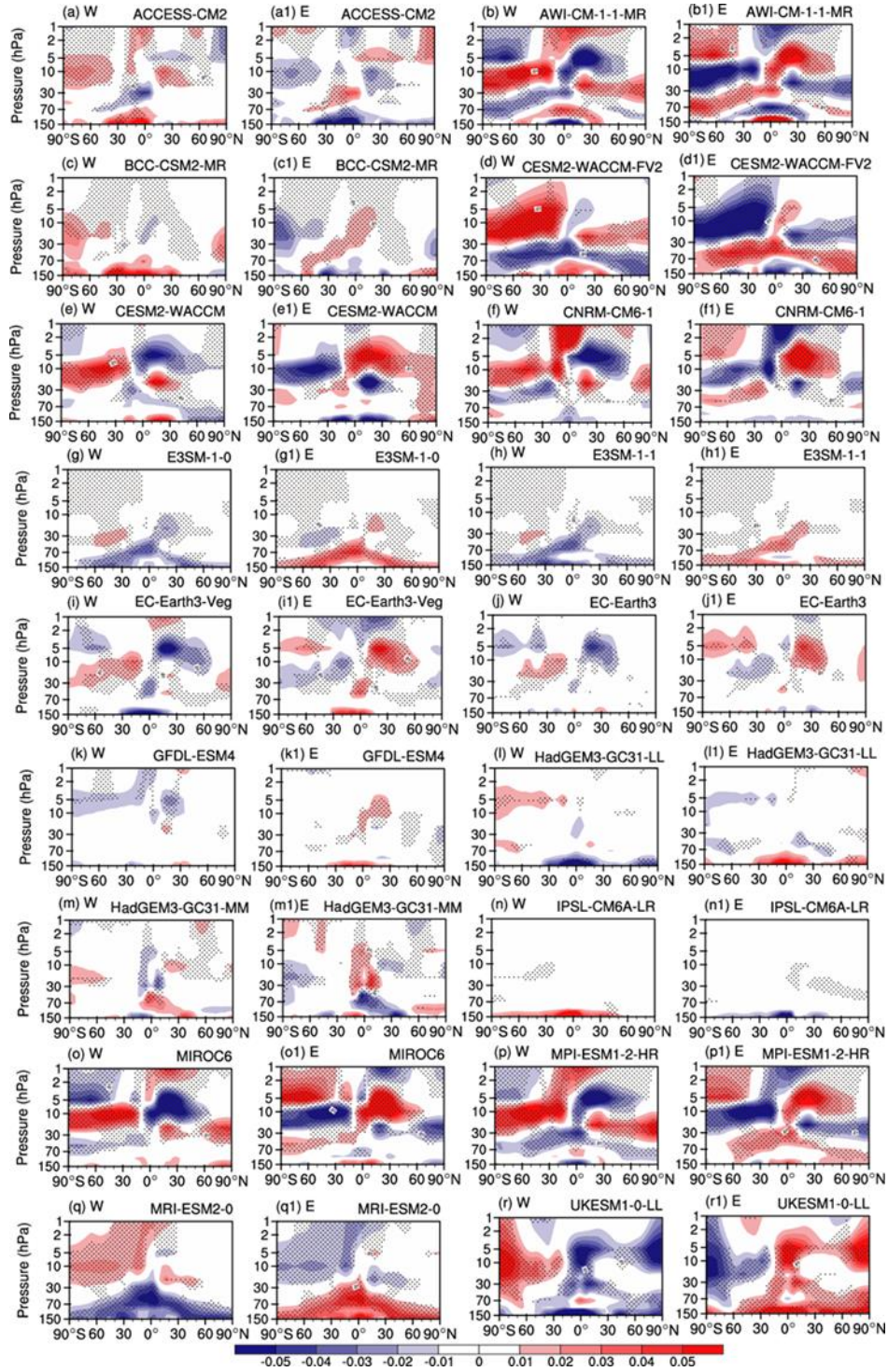


Figure S9. As in Figure S7, but for composite water vapor anomalies under different QBO phases in the northern winter (unit: ppm), respectively, for 18 CMIP6 models from 1959–2014.

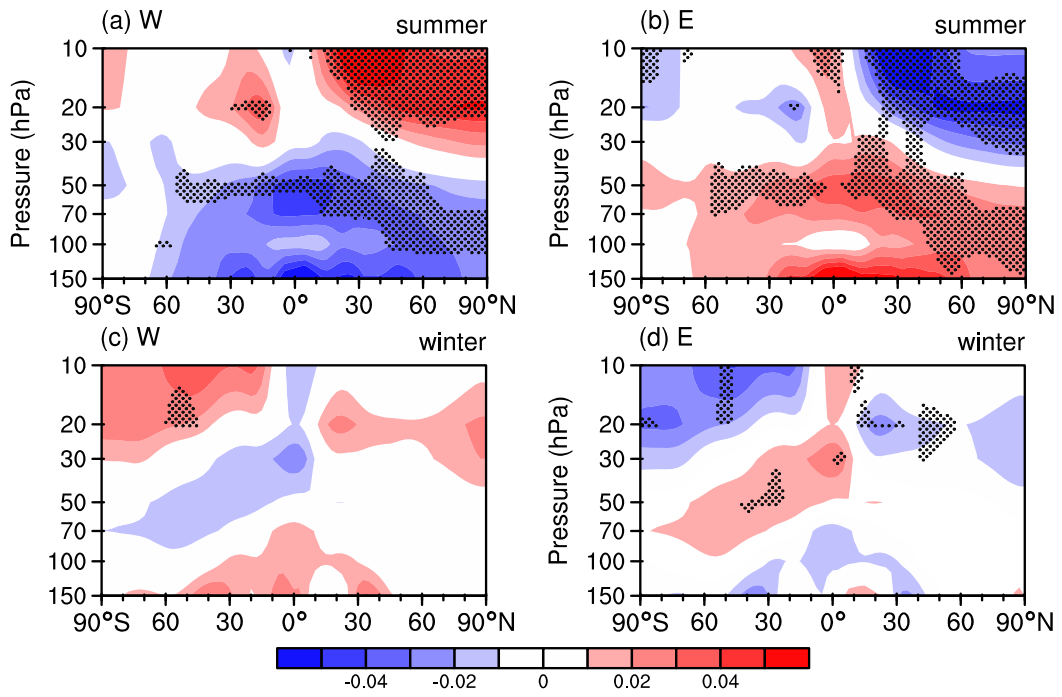


Figure S10. Composite of the 5 CMIP6 models in northern summer and 7 CMIP6 models in winter under different QBO phases from 1959–2014.